Available online at www.sciencedirect.com
SCIENCE DIRECT®
International Journal of Mass Spectrometry 233 (2004) 395–403
International Journal of Mass Spectrometry
www.elsevier.com/locate/ijms

Vacuum ultraviolet emissions from a cylindrical dielectric barrier discharge in neon and neon–hydrogen mixtures

N. Masoud [a], K. Martus [b], K. Becker [a,c,*]

[a] *Department of Physics, Stevens Institute of Technology, Hoboken, NJ 07030, USA*
[b] *Department of Chemistry and Physics, William Paterson University, Wayne, NJ 07470, USA*
[c] *Center for Environmental Systems, Stevens Institute of Technology, Hoboken, NJ 07030, USA*

Received 1 December 2003; accepted 1 February 2004

Abstract

The vacuum ultraviolet (VUV) emissions from a cylindrical dielectric barrier discharge (C-DBD) excited by radio frequency (rf) power at 13.56 MHz in both pure Ne and in a mixture of Ne and H_2 were analyzed. Measurements of the relative emission intensity of the Ne resonance lines and the Ne_2^* excimer continua in pure neon were studied as a function of pressure, rf power, and gas flow rate. In Ne–H_2 mixtures, we studied the emission of the H Lyman-α line as a function of H_2 concentration, pressure, gas flow rate, and rf power. The observed dependence of the VUV emissions on the gas pressure, net rf power, gas flow rate and, in the case of the spectra of the Ne–H_2 plasma, the H_2 concentration is explained on the basis of a detailed microscopic analysis of the excimer formation and destruction processes and the competition between the vibrational relaxation processes, quenching processes, and the radiative decay of two excimer states involved.

Keywords: Discharge plasma; Excimer emission; Neon; Hydrogen; Lyman-α line

1. Introduction

Light sources emitting intense radiation in the vacuum ultraviolet (VUV) region of the electromagnetic spectrum (wavelengths below about 200 nm) are used in a variety of applications such as photolithography, surface cleaning, curing, and sterilization and decontamination [1]. Plasma-based VUV light sources have several advantages over other sources. They are compact, efficient, easily scaleable, and the emitted wavelengths can be changed readily by simply changing the feed gas or gas mixture. Plasmas generated in various dielectric barrier discharges (DBDs) have been widely used for a long time as a convenient source of non-coherent ultraviolet (UV) and VUV radiation. In particular, high-pressure DBDs (with pressures up to and exceeding atmospheric pressure) are well-known sources of excimer emissions from rare gases and from rare gas-halide mixtures [2].

Recently, we have studied VUV emissions from microhollow cathode discharges in high-pressure Ne–H_2 gas mixtures and found, for a narrow range of operating conditions, intense monochromatic H Lyman-α emissions. This emission, which had first been reported by Wieser et al. [3] following excitation of a high-pressure Ne–H_2 mixture in a gas cell by energetic electrons, was attributed to a resonant energy transfer between Ne_2^* excimers formed in the plasma and H_2 molecules. The energy transfer leads to the dissociation of H_2 into a ground state H ($n = 1$) atom and an excited H ($n = 2$) atom, which subsequently decays radiatively emitting the H Lyman-α line. The production of hydrogen Lyman-α from an H_2 molecule requires a total energy of 14.68 eV, with 4.48 eV needed to dissociate H_2 and 10.2 eV needed to excite one H atom to the $n = 2$ state. The total energy for the production of Lyman-α coincides with a wavelength of 84.5 nm, which is near the maximum of the Ne_2^* second excimer continuum emission [4]. The most convincing argument for this explanation was the observation by Kurunczi et al. [4] that the Ne_2^* second excimer continuum emission intensity essentially disappeared when the H Lyman-α emission was observed.

One of the disadvantages of the microhollow cathode discharge source is the fact that the electrodes are exposed directly to the plasma, which causes erosion of the electrodes

* Corresponding author. Tel.: +1-201-216-5671; fax: +1-201-216-5638.
E-mail address: kbecker@stevens.edu (K. Becker).

1387-3806/$ – see front matter © 2004 Elsevier B.V. All rights reserved.
doi:10.1016/j.ijms.2004.02.007

and the dielectric that separates the electrodes [5]. As a consequence, the discharge performance deteriorates over time because the size of the hollow increases, which makes it more difficult to stabilize the discharge at high pressure. Furthermore, sputtering of the electrodes and the dielectric produces impurities thus reducing the efficiency of excimer formation [6]. Laroussi et al. [7] introduced a cylindrical dielectric barrier discharge (C-DBD), which avoids these problems by placing two electrodes around the outside of a dielectric tube. When radio frequency (rf) power is applied to the electrodes, an intense plasma is generated inside the tube in the space between the electrodes. This discharge plasma, when ignited in a high-pressure Ne–H_2 mixture, was found to be an efficient, intense, and highly stable (over more than 100 h) source of H Lyman-α radiation.

In this paper, we report the results of systematic investigations of the VUV emissions from a C-DBD source in pure Ne and in Ne–H_2 mixtures. Emissions of the Ne resonance lines at 73.6 and 74.4 nm and of the Ne_2^* excimers in the region from 76 to 90 nm were studied as a function of pressure, rf power, and gas flow rate in pure Ne discharges. In Ne–H_2 mixtures, we studied the H Lyman-α line emission as a function of H_2 concentration, total pressure, rf power, and gas flow rate. A comparison is made with similar results obtained previously from microhollow cathode discharge plasmas in Ne and Ne–H_2 [4,8].

2. Experimental setup

The discharge source is made of a 1/4 in. diameter dielectric tube (alumina, Al_2O_3) and two straps of Cu wrapped around it, separated by a fixed distance (2.5 mm), which serve as the two electrodes. A 13.56 MHz rf power generator, capable of delivering up to about 100 W, is applied to the two electrodes. The power source generates and sustains a stable discharge plasma inside the tube that is limited to the space between the electrodes. The feed gas or gas mixture is introduced into the tube and the gas flow is controlled by flow meters in order to maintain a constant overall gas pressure (and H_2 concentration when Ne–H_2 are used). In order to maximize the power that the rf generator delivers into the plasma, a matching network is used to match the impedance of the load (the plasma) with the output impedance of the generator.

Because the Ne resonance line radiation and the Ne_2^* excimer emission occur in the 70–100 nm range, where no material transmits optical radiation, a windowless arrangement was used between the plasma source and the vacuum monochromator/detector system. Fig. 1 shows the experimental setup that was used. The system is differentially pumped using multiple pumping stations to maintain a reduced pressure inside the vacuum monochromator and the CCD camera. The pressure inside the CCD camera never exceeded 10^{-5} Torr, when the gas pressure inside the discharge chamber varied from 1 to 600 Torr. The actual pressure in the discharge source can be lower depending on the source temperature (see discussion in Section 3.2). Using mass flow valves, the gas flow rate could be varied from 200 to 1200 sccm. The optical emissions were analyzed using a Minuteman 302-V 0.2 m VUV spectrometer with a McPherson XUV-2025 CCD camera to detect the photons in the wavelength range from 50 to 150 nm.

Since the efficiency of excimer formation depends (among other things as discussed below) critically on the purity of the feed gas, research grade neon and hydrogen gas was used with a stated purity of 99.999% in conjunction with stainless-steel gas lines. The inside of the discharge chamber was evacuated to a base pressure in the 10^{-7} Torr range for

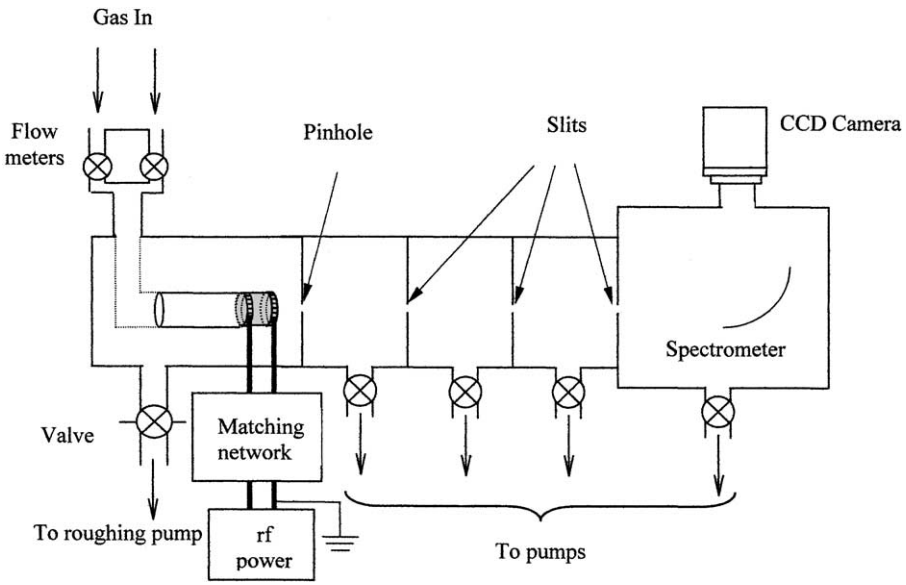

Fig. 1. Experimental setup.

at least 24 h before the source was back filled with the feed gas prior to data acquisition.

3. Results and discussion

3.1. Neon resonance lines and excimers

The most prominent VUV emissions that are observed from a low-pressure Ne plasma are the Ne resonance lines at 73.59 and 74.37 nm, which arise from radiative transitions from respectively the excited "$^1P_1$" and "$^3P_1$"states to the $^1S_0$ ground state. The quotation marks indicate that the excited states cannot be described in an LS angular momentum coupling scheme, but are more appropriately described in an intermediate angular momentum coupling scheme [9]. Alternatively, the excited "$^1P_1$" and "$^3P_1$" states of the rare gases are often described as mixtures of LS-coupled singlet and triplet states and the radiative decay of both states proceeds through the singlet component. The singlet–triplet mixture depends on the particular excited states and the particular rare gas atom [10]. In Ne, the first excited singlet state has about a 10% triplet admixture and vice versa [11]. The natural lifetime of the "$^1P_1$" and "$^3P_1$" states are 1.87 ns and 31.7 ns, respectively [12].

As the pressure in a Ne plasma increases, molecular excimer emissions begin to appear. Rare gas molecules exist only in the form of excimers (exotic *dimers*), which are characterized as having repulsive ground states that are dissociative and bound excited states. Transitions from the bound excited states of a rare gas excimer to the repulsive ground state results in continuous emissions. Rare gas excimer emission spectra are dominated by the so-called second continuum which corresponds to transitions from the lower vibrational levels of the lowest lying bound $^3\sum_u$ excimer state to the repulsive ground state with peak emissions at 170 nm (Xe), 145 nm (Kr), 130 nm (Ar), 84 nm (Ne), and 75 nm (He). The so-called first excimer continua in the rare gases are observed on the short-wavelength side of the second continua and are due to the radiative decay of vibrationally excited levels of the $^1\sum_u$ excimer state. In Ne, the second excimer continuum covers the wavelength range from 76 to 88 nm, whereas the first excimer continuum appears as a narrow feature centered between 73 and 75 nm [13–15].

The most common routes to rare gas excimer formation are either via electron-impact ionization of the rare gas atoms followed by a sequence of collision processes producing metastable rare gas atoms or directly via excitation of metastable (and radiative) states of the atom by electrons. In both cases, the excimer molecules are formed in three-body collisions involving a metastable rare gas atom and two ground-state atoms. Excimers are formed in a distribution of vibrational states of the excited $^1\sum_u$ and $^3\sum_u$ states. In Ne, the triplet state has a lifetime on the order of about 10 μs while that of the singlet state is in the range of nanoseconds [12]. Efficient excimer formation requires

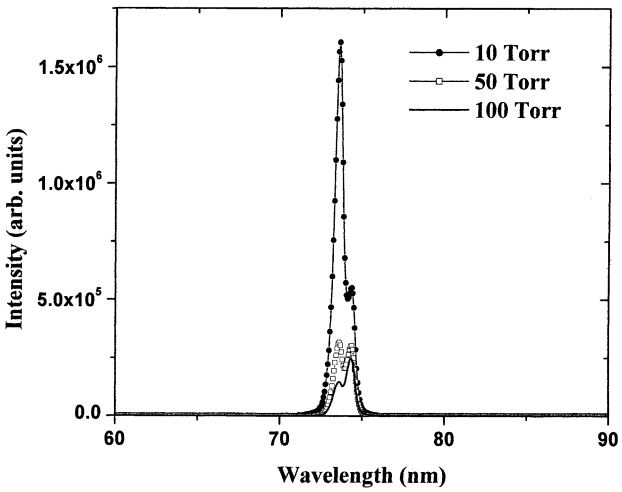

Fig. 2. Low-pressure spectrum of a Neon discharge at 10, 50 and 100 Torr in the 60–90 nm region. The net rf power is 30 W and the gas flow rate is 800 sccm. The lines connecting the data points are just a guide to the eye.

(i) a sufficiently large number of electrons with energies above the threshold for the metastable excitation or ionization (minimum electron energies required for excimer formation range from 11 to 14 eV in Xe to 20–24 eV in He), and (ii) a pressure that is high enough to have a sufficiently high rate of three-body collisions. These conditions exist in non-thermal, high-pressure discharge plasmas.

3.2. VUV emissions from a rf C-DBD plasma in pure Ne

3.2.1. Ne resonance lines

Fig. 2 shows the emission spectrum of a pure Neon discharge in the wavelength range from 60 to 90 nm obtained at pressures of 10, 50, and 100 Torr. The spectra are dominated by the Ne resonance lines. There is no indication in the spectra of Ne excimer emissions. At these low pressures the rate for three-body collisions involving metastable Ne atoms, which would lead to excimer formation, is much smaller than rates for two-body collisions that cause quenching of the Ne metastables. Thus, the radiative decay of the "$^1P_1$" and $^3P_1$ states is the dominant process.

The ratio of "singlet" (73.6 nm) to "triplet" (74.6 nm) emission intensity changes dramatically as a function of pressure. At 10 Torr, the 73.6 nm line is about three times as intense as the 74.6 nm line. At 50 Torr, the intensity of the lines are roughly equal. However, the overall intensity at 50 Torr is lower than the overall intensity at 10 Torr. At 100 Torr, both lines are much weaker and the 74.6 nm line is now more intense than the 73.6 nm line by about a factor of 2. This change in the emission intensity with pressure is a consequence of self-absorption and radiation trapping of the Ne resonance radiation, which affects the 73.6 nm line to a much larger extent because of its higher transition probability. The intensity ratio of the two Ne resonance lines emitted from a C-DBD plasma in pure Ne as a function of pressure is shown in Fig. 3 from 5 Torr (the lowest pressure

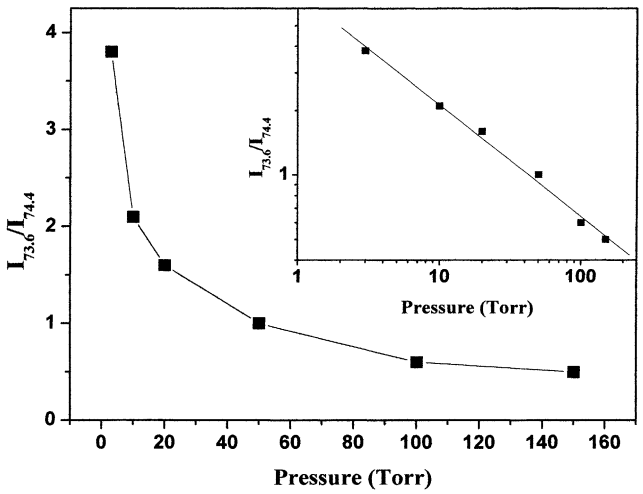

Fig. 3. Intensity ratio of the Ne resonance lines as a function of pressure. The net rf power is 30 W and the gas flow rate is 800 sccm. The lines connecting the data points are just a guide to the eye. The inset represents the same data on a log–log scale with the line representing a least-squares fit to the data.

at which we could maintain a stable discharge in our source) to 150 Torr. The inset shows the same data plotted on a log-log scale, which shows a straight line with a slope of essentially −0.5. Thus, the intensity ratio of the 73.6 nm line to the 74.4 nm line is inversely proportional to the square root of the pressure. We lastly note, that even at a pressure of 5 Torr, significant radiation trapping and quenching occurs as the intensity ratio of the two lines when excited by electron impact at very low pressure, i.e., under single collision conditions is close to 17.

3.2.2. Ne excimer emission

At pressures above 200 Torr, we find no discernible evidence of the presence of the Ne resonance lines in the spectrum obtained from our source and the Ne_2^* excimer emissions in the 70–90 nm region become the dominant feature. This is due to the fact that the rate for three-body collisions involving Ne metastables leading to excimer formation begins to dominate over the rates for two-body quenching collisions. Fig. 4 shows the emission spectra obtained from a pure Ne discharge (at a net power of about 30 W and a gas flow rate of 800 sscm) for pressures of 400, 500, and 600 Torr. The spectra are dominated by the narrow first excimer continuum peaking at a wavelength of about 74 nm and by the broad second excimer continuum, which covers the wavelength region from 76 to 88 nm with a peak emission at about 84 nm.

3.2.2.1. Pressure dependence. Fig. 5 shows the emission intensities of the first and second Ne_2^* excimer continua as a function of gas pressure from 200 to 600 Torr. The data represents the peak areas of the continua, which were obtained from the recorded data with the help of a standard peak fitting software package (PEAKFIT^{TM} version 4.11, SYSTAT Software Inc., 2002). It is apparent from Figs. 4 and 5 that the emission intensities of first and second continua are a function of the gas pressure, in particular the emission intensity of the first excimer continuum decreases monotonically by more than a factor of 25 as the pressure increases from 200 to 600 Torr. By contrast, the emission intensity of the second continuum increases by about 30% as the pressure increased from 200 to 400 Torr. However, as the pressure is increased further, the emission intensity of

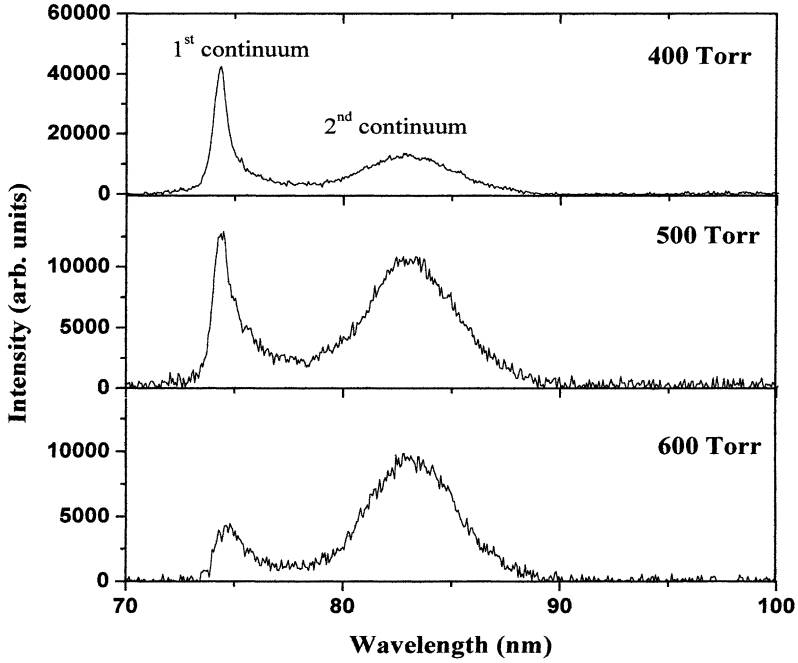

Fig. 4. High-pressure spectrum of a Neon discharge at 400, 500 and 600 Torr. The net rf power is 30 W and the gas flow rate is 800 sccm.

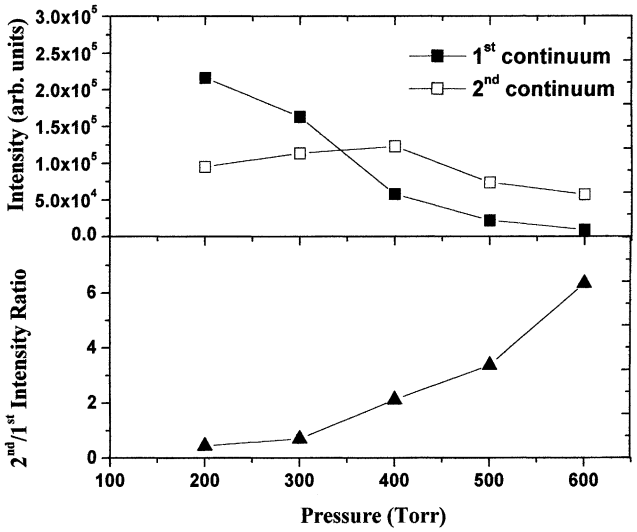

Fig. 5. Emission intensity of the first, the second Neon excimer continua and their ratio as a function of gas pressure above 200 Torr at a net rf power of 30 W and a gas flow rate of 800 sccm. The lines connecting the data points are just a guide to the eye.

the second continuum also decreases, by more than a factor of 2 between 400 and 600 Torr. The ratio of the emission intensity of the second continuum to that of the first continuum increases monotonically as the pressure increases from 200 to 600 Torr. The increase in the ratio from 200 to 400 Torr is the result of an increasing intensity of the second continuum and a decreasing intensity of the first continuum. At higher pressures, both emission intensities decrease with increasing pressure, but the intensity of the first continuum declines faster with increasing pressure compared to the intensity of the second continuum.

The pressure dependence of the two Ne_2^* excimer emission continua shown in Figs. 4 and 5 is similar to what was observed by other authors investigating Ne_2^* excimer emissions from a variety of sources such as high-pressure Ne gas excited by energetic electron or ion impact [12,15] and other high-pressure discharge plasmas including DBDs and microhollow cathode discharges [4,16,17]. All groups reported a dominant (in terms of its peak height) first excimer continuum at pressures below about 400 Torr, which is quenched very efficiently at pressures above 400 Torr. For higher pressures, the emission spectrum is dominated by the second continuum, whose overall emission intensity peaks around 400 Torr and declines gradually as the pressure is increased further. This can be understood from the detailed microscopic analysis of the excimer formation where the decay of the upper vibronic states proceed through two pathways, collisional de-excitation to low-lying vibronic states of the excimer and radiatively to the dissociative ground state. The vibrational relaxation process to the lower-lying vibronic states depends on the collision frequency (i.e., pressure). Therefore, at low pressure the collision frequency is low and the vibrational relaxation time is large, so that the dominant decay process is radiative to the ground state leading to the emission of the first continuum. If the pressure increases, the collision frequency increases, the relaxation time for the collisional pathway decreases, and the lower-lying vibronic states are populate and subsequently decay to the ground state emitting the second continuum. The decline in the intensity of the second continuum at higher pressures (>400 Torr) is attributed to the fact that, at these pressures, the gas density is very high, so that both the excited Ne atoms, which are the precursor of the Ne_2^* excimer, and the excimer molecules are quenched.

3.2.2.2. Power dependence. Fig. 6 shows the emission intensity of the two Ne_2^* excimer continua as a function of the rf power for net powers deposited in the plasma ranging from 15 to 70 W at a pressure of 500 Torr and a gas flow rate of 800 sccm. The intensity of the first continuum increases as the power goes up, initially at low powers only gradually, but more dramatically above about 50 W. On the other hand, the intensity of the second continuum increases almost linearly between 15 and 50 W, but then levels off for higher powers. As a consequence, the ratio of the emission intensity of the second to the first continuum decreases monotonically between 15 and 70 W. The increase in the excimer emission intensity with increasing power corresponds to an increase in the electron density and a shift in the average electron energy to higher values. Thus, an increase in power leads to an increase in the rate of metastable Ne formation, which are the precursors of the Ne_2^* excimers.

We attribute the different rate of increase in the emission intensity with power for respectively the first and second excimer continuum to the fact that the gas temperature increases with increasing rf power. We found that the gas temperature increases from about 340 to 410 K when the power increases from 15 to 60 W [18]. An increase of the gas temperature at constant pressure reduces the gas density and thus the pressure inside the plasma source (which then is lower than the recorded pressure in the discharge chamber). At a nominal pressure of 500 Torr in the discharge chamber, a lower pressure at higher power inside the plasma source will cause an increase in the intensity of both excimer continua, but at a different rate (see Fig. 5).

3.2.2.3. Gas flow rate dependence. Fig. 7 shows the emission intensities of the first and second continua emitted from a Ne plasma at a pressure of 500 Torr excited by a rf power of 30 W as a function of the gas flow rate. An increase of the Ne gas flow rate causes very little change in the emission intensity of the first continuum (which is almost independent of the flow rate), but a distinct increase of the intensity of the second continuum. A possible explanation for this behavior is the fact that the flowing gas carries away impurities. The intensity of the second excimer continuum is particularly sensitive to quenching collisions with impurities because of the long radiative lifetime of the emitting state. Thus, reducing the impurities by increasing

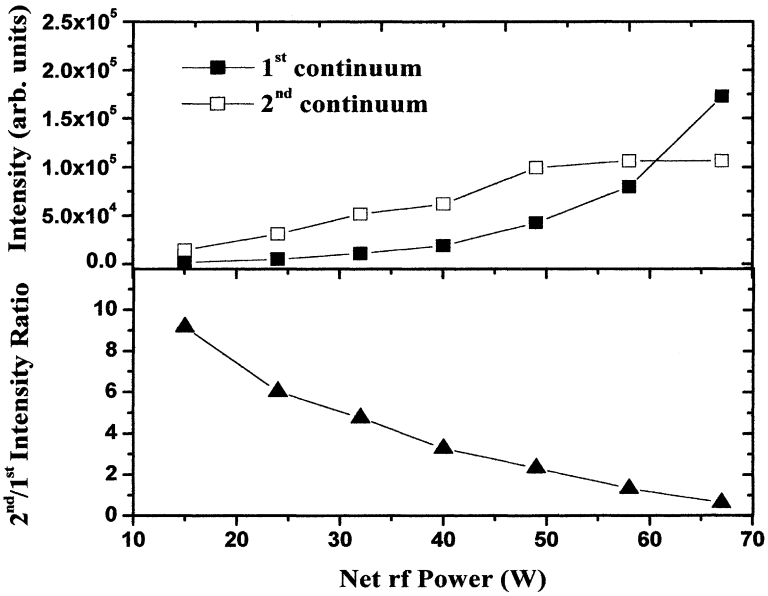

Fig. 6. Emission intensity of the first, the second Neon excimer continua and their ratio as a function of the net rf power at a pressure of 500 Torr and a gas flow rate of 800 sccm. The lines connecting the data points are just a guide to the eye.

the flow rate will result in less efficient quenching and an increase in the intensity of the second continuum.

3.2.2.4. The third Ne_2^* excimer continuum. In addition to the prominent first and second Ne excimer continua, there is also a third continuum, which has been observed by authors [14,15,19], mainly following bombardment of high-pressure rare gases by energetic electron or ion beams. Even though the third continuum has rarely been observed in high-pressure rare gases discharge plasmas, we established a range of operating parameters, of our rf C-DBD plasma in Ne, for which the third continuum can be observed. At a pressure between 200 and 250 Torr and at comparatively low power, the Ne_2^* third excimer continuum appears at wavelengths between 92 and 105 nm as shown in Fig. 8. The origin of the third continuum is still a subject of debate. Langhoff [19] assigned the third excimer continuum to an emission associated with the radiative decay of the doubly charged Ne_2^{2+} ion into two singly charged Ne ground-state atoms. Amirov et al. [20] proposed a highly-excited singly

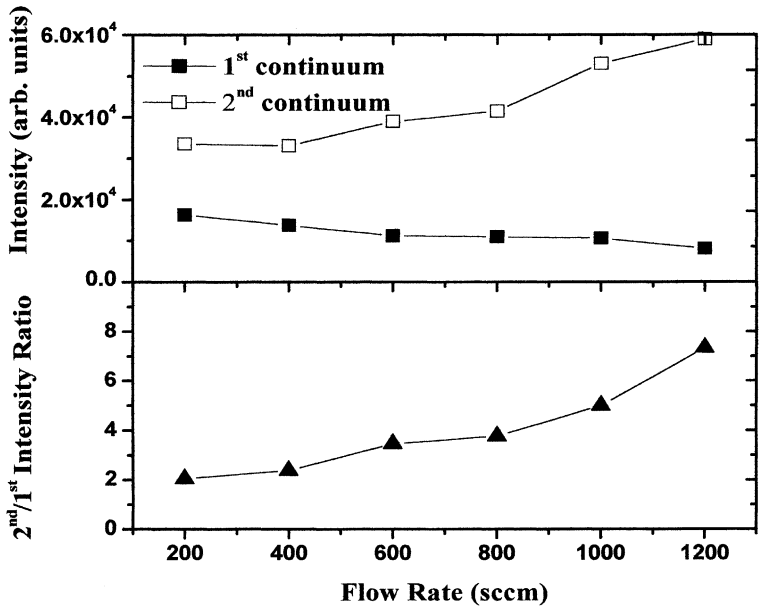

Fig. 7. Emission intensity of the first, the second Neon excimer continua and their ratio as a function of the gas flow rate at a net rf power of 30 W and a gas pressure of 500 Torr. The lines connecting the data points are just a guide to the eye.

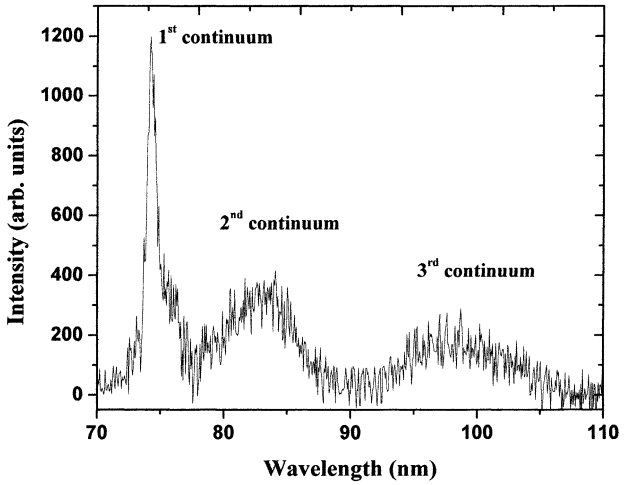

Fig. 8. Third Ne excimer continuum shown in the emission spectrum of a Ne discharge (pressure 250 Torr, gas flow rate 800 sccm, and net rf power 15 W).

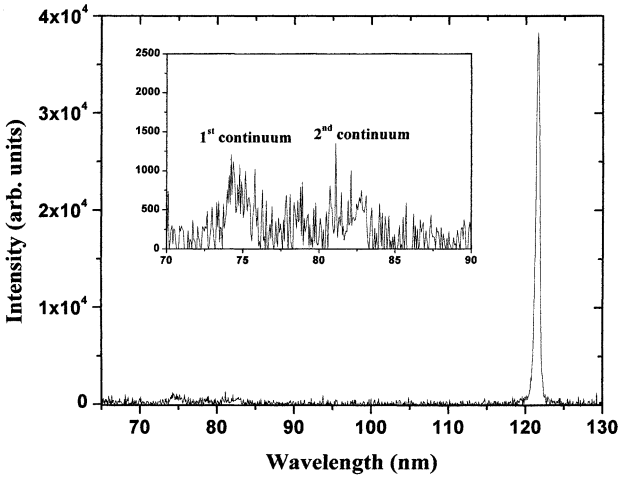

Fig. 9. The emission spectrum of a neon discharge with a small admixture of hydrogen (0.02%) at a total pressure of 500 Torr, a flow rate of 800 sccm and a net rf power of 30 W. The inset shows the expanded view of the spectrum in the 70–90 nm region.

charged rare gas ion as the origin of the third continuum emission. It is interesting to note that the emission of the third continuum from our source could only be observed in a narrow pressure range (200–250 Torr). This is similar to an observation by Leichner [12], who found a broad continuum emission peaked at around 100 nm at a pressure around 100 Torr, which disappeared at 500 Torr in their experiments.

3.3. VUV emissions from a rf C-DBD plasma in a Ne–H_2 mixture

Similar to what was done before in the experiments reported by Wieser et al. [3] (e-beam excitation of a high-pressure Ne–H_2 mixture) and Kurunczi and coworkers [4,8] (excitation of a high-pressure Ne–H_2 mixture in a micro-hollow cathode discharge plasma), we studied the VUV emissions from the rf excited C-DBD plasma in a high-pressure Ne–H_2 mixture. The objective was to investigate the resonant energy transfer between the Ne_2^* second excimer continuum and H_2 molecules leading to the emission of a monochromatic H Lyman-α line in this device and to extend the earlier investigation of El-Dakrouri et al. [21] to a simultaneous analysis of the Ne_2^* excimer emission and the H Lyman-α emission. Fig. 9 shows the emission spectrum from our source obtained by adding a small amount of hydrogen (0.02%) to Ne at a total pressure of 500 Torr, a total gas flow rate of 800 sccm, and a net rf power of 30 W. Compared with the previous spectrum obtained in pure Ne (Fig. 4), we see a dramatic decrease in the relative intensity of the second continuum accompanied by the emission of a very intense, monochromatic H Lyman-α line. We subsequently studied the dependence of the H Lyman-α emission intensity on the pressure, the net rf power, the gas flow rate, and the H_2 concentration.

3.3.1. Pressure dependence

Fig. 10 shows the intensity of H Lyman-α line as a function of pressure for a net rf power of 30 W and a H_2 concentration of 0.1%. Under these conditions, the Lyman-α emission intensity rises almost linearly up to a pressure of 200 Torr, where the intensity has its maximum. For higher pressures, the Lyman-α intensity was found to decrease, but it still dominates the emission spectra. The increase of the Lyman-α emission with increasing pressure follows the increase of the Ne_2^* second continuum intensity, which is the precursor of the Lyman-α emission, with pressure (Fig. 5). The fact that the Lyman-α emission intensity reaches its maximum already at 200 Torr as compared to 400 Torr for the second continuum can be explained by the fact that the peak emission intensity of the second continuum at 400 Torr was obtained in a pure Ne plasma. The addition of H_2 to the

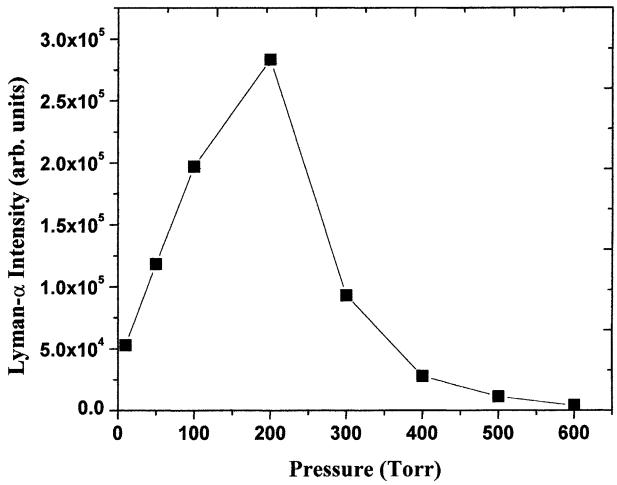

Fig. 10. The intensity of Lyman-α radiation as a function of pressure at a net rf power of 30 W and a H_2 concentration of 0.1%. The lines connecting the data points are just a guide to the eye.

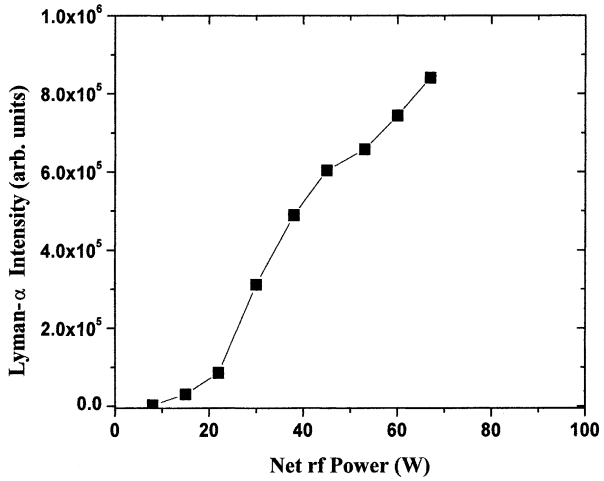

Fig. 11. The Lyman-α line intensity as a function of the net rf power at 200 Torr, 0.1% H_2 and 800 sccm flow rate. The lines connecting the data points are just a guide to the eye.

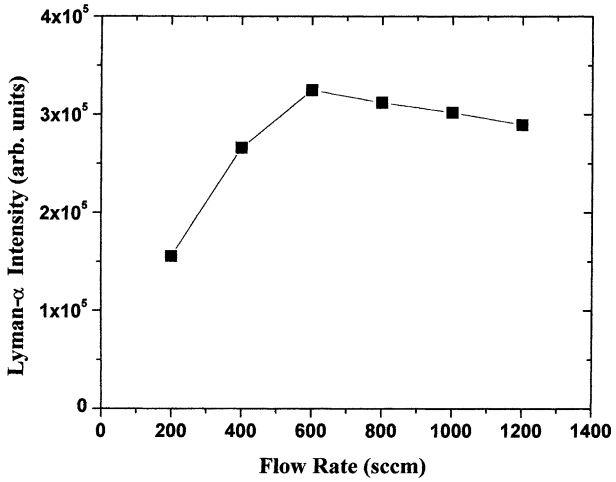

Fig. 12. The Lyman-α line intensity as a function of the gas flow rate at 200 Torr, 0.l% H_2 and 30 W net rf power. The lines connecting the data points are just a guide to the eye.

feed gas mixture essentially means introducing impurities, which will reduce the efficiency of excimer formation, e.g., by quenching the excimer precursors.

3.3.2. Power dependence

Fig. 11 shows the Lyman-α line intensity as a function of the rf power for a total pressure of 200 Torr, a gas flow rate of 800 sccm, and a 0.1% H_2 admixture. The intensity of the line emission increases monotonically as the power is increased. It is interesting to note that the Lyman-α intensity even increases for rf powers above 50 W, where the intensity of the second continuum as a function of rf power levels off (Fig. 6). This may be explained by the fact that other mechanisms such as ionization of H_2 by Ne metastables followed by dissociative recombination or energy transfer from the Ne_2^* first excimer continuum may also contribute to the formation of H ($n = 2$) atoms in our plasma.

3.3.3. Gas flow rate dependence

Fig. 12 shows the dependence of the Lyman-α line intensity on the total gas flow rate obtained from a 30 W plasma at 200 Torr with a 0.1% H_2 concentration. The intensity increases with increasing gas flow rate up to 600 sccm and then stays essentially constant at higher flow rates. This dependence corresponds to the flow rate dependence of the second continuum (Fig. 7) except for the shift in the value of the flow rate at which the intensity levels off, at around 1000 sccm for the second continuum compared to around 600 sccm for the Lyman-α line.

3.3.4. H_2 concentration dependence

The Lyman-α intensity increases with increasing H_2 concentration up to concentrations of 0.05% as shown by the data in Fig. 13, which were obtained at a pressure of 200 Torr, a gas flow rate of 800 sccm, and a net rf power of 30 W. As the H_2 concentration is increased above 0.05%,

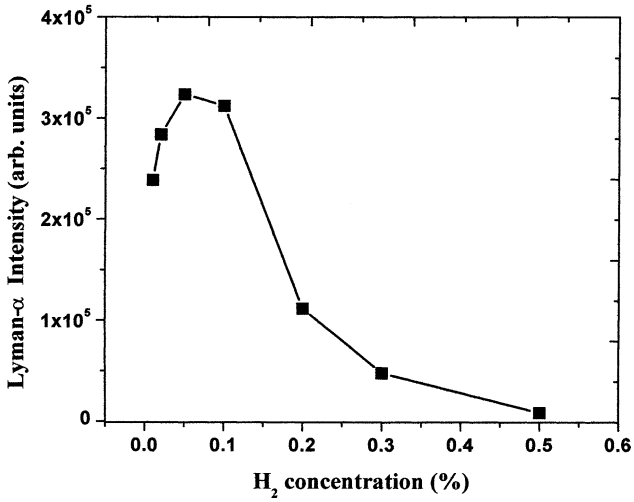

Fig. 13. The Lyman-α line intensity as a function of H_2 concentration at 200 Torr, 800 sccm flow rate and 30 W net rf power. The lines connecting the data points are just a guide to the eye.

the Lyman-α emission intensity begins to drop. At a H_2 concentration of 0.5% the Lyman-α intensity has dropped to less than 3% of its peak value. A similar behavior was observed by Kurunczi [8] in the case of the Lyman-α emission from a microhollow cathode discharge and was attributed to the increase in the H_2 number density in the plasma at H_2 concentration about 0.05%. This causes (i) efficient quenching of the Ne metastables which reduces the formation of the Ne_2^* excimers and (ii) the formation of ground-state H atoms via dissociation of H_2, which cause self-absorption and trapping of the Lyman-α emission.

4. Conclusions

The VUV spectra of the neon resonance lines, neon excimers and their energy transfer to H_2 has been studied in a

high pressure rf excited C-DBD source for pressures up to 600 Torr. The observed dependence of the VUV emissions on the gas pressure, net rf power, gas flow rate and the H_2 concentration has been explained on the basis of a detailed microscopic analysis of the excimer formation and destruction processes and the competition between the vibrational relaxation processes, quenching processes, and the radiative decay of two excimer states involved. When ignited in a high-pressure Ne–H_2 mixture, the C-DBD source was found to be an efficient, intense, and highly stable source of H Lyman-α radiation. The low cost of the C-DBD source as well as the simplicity in both the fabrication and control of the operating conditions such as pressure, power, and flow rate and hence the intensity of the emitted light give the source many advantages over the other sources.

Acknowledgements

This work was supported by the US National Science Foundation (NSF). One of us (K.M.) wishes to thank the William Paterson University Sabbatical Leave program for the opportunity to undertake this project. We would like to thank Prof. M. Laroussi and Dr. P. Kurunczi for many helpful discussions.

References

[1] A. Bogaerts, E. Neyts, R. Gijbels, J. van der Mullen, Spectrochim. Acta B: At. Spectrosc. 57 (4) (2002) 609.
[2] I.W. Boyd, J.Y. Zhang, NIMB 121 (1997) 349.
[3] J. Wieser, M. Salvermoser, L.H. Shaw, D.E. Murnick, H. Dahi, J. Phys. B: At. Mol. Opt. Phys. 31 (1998) 4589.
[4] P. Kurunczi, H. Shah, K. Becker, J. Phys. B: At. Mol. Opt. Phys. 32 (1999) L651.
[5] K.H. Schoenbach, A. El-Habachi, W. Shi, M. Ciocca, Plasma Sour. Sci. Technol. 6 (1997) 468.
[6] A. El-Habachi, W. Shi, M.M. Moselhy, R.H. Stark, K.H. Schoenbach, J. Appl. Phys. 88 (6) (2000) 3220.
[7] M. Laroussi, in: Proceedings of IEEE International Conference on Plasma Science, Monterey, CA, 1999, p. 203.
[8] P. Kurunczi, Ph.D. Thesis, Stevens Institute of Technology, unpublished.
[9] I.I. Sobelman, Atomic Spectra and Radiative Transitions, Springer Verlag, Heidelberg, 1979.
[10] K. Bartschat, D.H. Madison, J. Phys. B: At. Mol. Phys. 20 (1987) 5839.
[11] I. Kanik, J.M. Ajello, G.K. James, J. Phys. B: At. Mol. Opt. Phys. 29 (1996) 2355.
[12] P.K. Leichner, Phys. Rev. A 8 (2) (1973) 815.
[13] K. Petkau, J.W. Hammer, G. Herre, M. Mantel, H. Langhoff, J. Chem. Phys. 94 (12) (1991) 7769.
[14] T. Grieget, H.W. Drotleff, J.W. Hammer, K. Petkau, J. Chem. Phys. 93 (7) (1990) 4581.
[15] W. Krotz, A. Ulrich, B. Busch, G. Ribitzki, J. Wieser, Appl. Phys. Lett. 55 (22) (1989) 2265.
[16] B. Eliasson, M. Hirth, U. Kogelschatz, J. Phys. D: Appl. Phys. 20 (1987) 1421.
[17] B. Eliasson, U. Kogelschatz, IEEE Trans. Plasma Sci. 19 (1991) 309.
[18] K. Martus, N. Masoud, K. Becker, Proceedings of 56th Gaseous Electronics Conference, San Francisco, CA, October 2003.
[19] H. Langhoff, Opt. Commun. 68 (1) (1988) 31.
[20] A.K. Amirov, O.V. Korshounov, V.F. Chinnov, J. Phys. B 27 (1994) 1753.
[21] A. El-Dakrouri, J. Yan, M.C. Gupta, M. Laroussi, Y. Badr, J. Phys. D: Appl. Phys. 35 (2002) L109.